Paleoceanography and Paleoclimatology

RESEARCH ARTICLE
10.1029/2022PA004543

# Abrupt Changes in Atmospheric Circulation During the Medieval Climate Anomaly and Little Ice Age Recorded by Sr-Nd Isotopes in the Siple Dome Ice Core, Antarctica

**Bess G. Koffman[1,2], Steven L. Goldstein[2,3], Gisela Winckler[2,3], Michael R. Kaplan[2], Louise Bolge[2], and Pierre Biscaye[2]**

[1]Department of Geology, Colby College, Waterville, ME, USA, [2]Lamont-Doherty Earth Observatory of Columbia University, Palisades, NY, USA, [3]Department of Earth and Environmental Sciences, Columbia University, New York, NY, USA

### Key Points:

- An ice core dust provenance record from Siple Dome shows marked shifts at about 1125 CE (lasting ~60 yr) and 1748 CE (~20 yr)
- Sr-Nd isotopes indicate changes in the relative deposition of dust from Patagonian and Antarctic sources driven by changes in winds
- Data suggest decade-scale changes can be superimposed on longer intervals of intensified westerly wind strength during SAM + -like phases

### Supporting Information:

Supporting Information may be found in the online version of this article.

### Correspondence to:

B. G. Koffman,
bess.koffman@colby.edu

### Citation:

Koffman, B. G., Goldstein, S. L., Winckler, G., Kaplan, M. R., Bolge, L., & Biscaye, P. (2023). Abrupt changes in atmospheric circulation during the Medieval Climate Anomaly and Little Ice Age recorded by Sr-Nd isotopes in the Siple Dome ice core, Antarctica. *Paleoceanography and Paleoclimatology*, *38*, e2022PA004543. https://doi.org/10.1029/2022PA004543

Received 6 SEP 2022
Accepted 13 MAR 2023

### Author Contributions:

**Conceptualization:** Bess G. Koffman, Steven L. Goldstein, Pierre Biscaye
**Data curation:** Bess G. Koffman
**Formal analysis:** Steven L. Goldstein
**Funding acquisition:** Bess G. Koffman
**Investigation:** Bess G. Koffman
**Methodology:** Bess G. Koffman, Louise Bolge, Pierre Biscaye
**Project Administration:** Steven L. Goldstein, Pierre Biscaye
**Resources:** Bess G. Koffman, Steven L. Goldstein, Pierre Biscaye
**Supervision:** Steven L. Goldstein, Gisela Winckler, Michael R. Kaplan
**Visualization:** Bess G. Koffman
**Writing – original draft:** Bess G. Koffman



## Abstract

The Southern Hemisphere westerly winds (SWW) play a critical role in global climate, yet their behavior on decadal to centennial timescales, and the mechanisms driving these changes during the preindustrial era, remain poorly understood. We present a decadally resolved record of dust compositions using strontium and neodymium isotope ratios in mineral dust from the Siple Dome ice core, Antarctica, to explore the potential that abrupt changes in SWW behavior occurred over the past millennium. The record spans portions of the Medieval Climate Anomaly (MCA) and the Little Ice Age (LIA) intervals as defined in the Northern Hemisphere. We find evidence of an abrupt strengthening of atmospheric circulation during the MCA at ~1125 CE (825 BP) that persisted for about 60 yr, indicating increased influence of Patagonia-sourced dust. This occurs during an extended positive phase of Southern Annular Mode (SAM+)-like conditions, characterized by high SWW velocities and a southerly shift of the main wind belt toward ~60°S, suggesting that rapid changes in SWW strength could occur under the present SAM+ pattern. A second 20 yr long shift in dust compositions during the LIA at ~1748 CE (200 BP) is coincident with higher dust delivery to Siple Dome, and may indicate increased dust emissions related to glacier activity in Patagonia. The new Siple Dome ice core data set demonstrates that Sr-Nd isotopes can be used to trace shifts in atmospheric circulation on decadal timescales.

## Plain Language Summary

The prevailing winds that encircle Antarctica, blowing west to east, play an outsized role in global climate. Because they blow continuously over the ocean, they create ocean currents and cause upwelling. When deep ocean water comes to the surface, it releases carbon dioxide into the atmosphere, causing the climate to warm. Changes in wind strength and positioning modulate the release of carbon dioxide. Therefore, knowing how and why the winds shift is important for understanding how Earth's climate system operates. We use the composition of dust preserved in an Antarctic ice core to learn how the balance of dust sources changed during the past millennium. This allows us to track past shifts in the winds around Antarctica and to learn how they respond to climate changes on short timespans, such as decades to centuries. We observe an abrupt change in dust composition at ~1125 CE lasting for about 60 yr, indicating a greater influence of dust sourced from Patagonia in South America. This dust shift occurred during a globally observed warm period, and corresponded with an interval of stronger westerly winds blowing closer to Antarctica. Our data show that decade-scale changes can be superimposed on longer intervals of intensified wind strength.

## 1. Introduction

The Southern Hemisphere westerly winds (SWW; Figure 1) are central to global climate dynamics, influencing the distribution of Southern Hemisphere mid-to-high latitude sea ice, moisture, and aerosols, and driving the ventilation of the Southern Ocean, which in turn modulates global atmospheric $CO_2$ and temperature (Anderson et al., 2009; Burke & Robinson, 2012; Toggweiler et al., 2006). Changes in their position are thought to directly drive changes in global climate through their influence on low-to-high-latitude ocean heat transport (Denton et al., 2021). Holocene proxy records from around the Southern Hemisphere including speleothems, glacier chronologies, and lake, marine, and bog cores, show a largely coherent pattern of SWW variability that correlates with $CO_2$ changes recorded by ice cores (Browne et al., 2017; García et al., 2020; Hall et al., 2019; Lamy et al., 2001; Moreno et al., 2018, 2014; Reynhout et al., 2022; Saunders et al., 2018; Schimpf et al., 2011; Xia et al., 2018).

**Writing – review & editing:** Bess G. Koffman, Steven L. Goldstein, Gisela Winckler, Michael R. Kaplan

While Holocene SWW and $CO_2$ variations have been relatively small compared to changes on glacial-interglacial timescales (Marcott et al., 2014; Moreno et al., 2018), studies of these recent fluctuations, and their drivers, are relevant for understanding and modeling carbon cycle dynamics during warm climate boundary conditions.

The Common Era (the past ~2,000 yr) provides the most recent pre-industrial examples of climate changes associated with changes in SWW behavior. Although their expression was spatially heterogeneous, changes in temperature and winds associated with the Medieval Climate Anomaly (MCA, ~850–1300 CE) and Little Ice Age (~1300–1850 CE) intervals are documented by Antarctic ice cores. For instance, during the MCA, the Ross Sea region (Figure 1) registered warmer temperatures (Bertler et al., 2011) accompanied by a weaker Amundsen Sea Low pressure center (ASL; Kreutz et al., 2000). During the LIA interval, ice cores from the western Ross Sea recorded temperature anomalies of −1.6°C ± 1.4°C (Erebus Saddle; Rhodes et al., 2012) and about −2°C (Lower Victoria Glacier; Bertler et al., 2011) relative to modern. In central West Antarctica, a West Antarctic Ice Sheet (WAIS) Divide ice core borehole showed a cooling of 0.52°C ± 0.28°C during 1400–1800 CE (Orsi et al., 2012). Cooler temperatures were accompanied by a strengthened ASL (Kreutz et al., 2000) and persistently strong katabatic winds in the Ross Sea sector (Rhodes et al., 2012). Because at least the lower elevations of Antarctica (e.g., WAIS and the Ross Sea region) experienced LIA cooling, high-resolution ice cores from these regions spanning the past ~1,200 yr allow for an assessment of changes in atmospheric circulation that may relate to SWW behavior across the MCA and LIA.

Atmospheric dust collected from ice cores serves as an indicator of past atmospheric circulation because its geochemical compositions carries information that reflects the dust's emission source. The radiogenic isotopes of strontium (Sr) and neodymium (Nd) are well-established tracers of dust source regions (Aarons et al., 2019; Delmonte et al., 2008, 2020; Grousset & Biscaye, 2005). While major dust suppliers in the Southern Hemisphere are characterized by some overlap in their Sr-Nd compositions (Delmonte et al., 2004; Koffman et al., 2021a), the consideration of likely transport pathways and additional geochemical information such as major, rare earth (REEs) and other trace elements can strengthen interpretations of source attribution (Koffman et al., 2021b). In this paper, we present a decadally resolved record of Sr-Nd isotopes from the Siple Dome ice core in the Ross Sea sector of Antarctica (Figure 1). The record, between ~1030–1202 CE and ~1665–1771 CE, spans portions of the MCA and LIA climate periods respectively (as defined in the Northern Hemisphere), allowing for an assessment of atmospheric circulation changes across these intervals.

## 2. Materials and Methods

The Siple Dome A deep ice core was drilled in the late 1990s, on a coastal ice dome located in the Ross Sea sector of West Antarctica (81.6667°S, 148.8167°W, 621 m a.s.l.; Figure 1). Dust samples were centrifuged in the 1990s from melted ice using a continuous-flow Sharples supercentrifuge, which operates at 30,000 RPM (Bory et al., 2002), and were stored in acid-cleaned beakers under cleanroom conditions. We assume these specific depth intervals (i.e., ~39–53 and 101–120 m) were targeted to provide a comparison of MCA and LIA periods. Ideally future work can extend the time series to obtain a more complete understanding of Late Holocene variability in dust provenance and associated changes in Southern Hemisphere atmospheric circulation.

Samples were digested for this project using HF-$HNO_3$ following standard procedures at the Lamont-Doherty Earth Observatory of Columbia University (LDEO; Koffman et al., 2021b). Each beaker contained visible dust grains, and the entirety of each sample was digested in order to make these low-level isotope measurements. Unfortunately, the exact volumes of ice contributing to each sample are no longer known. We measured 20 Sr and 24 Nd isotope ratios on a ThermoScientific Neptune Plus MC-ICP-MS at LDEO using static multi-collection. Procedural blanks yielded ≤41 pg Sr and ≤1 pg Nd, which are negligible compared to sample sizes. We assessed drift, fractionation, and reproducibility using international reference materials NIST SRM 987 (Sr; we used $^{87}Sr/^{86}Sr = 0.710240$) and JNdi (Nd; we used $^{143}Nd/^{144}Nd = 0.512115$ [Tanaka et al., 2000]). Repeat measurements of these standards, 10–30 per run, bracketed each sample and yielded 2$\sigma$ external errors for $^{87}Sr/^{86}Sr$ of ±0.000014 and ±0.000019 and for $^{143}Nd/^{144}Nd$ of ±0.000007 and ±0.000013 for two measurement intervals. Several samples of one analytical run experienced a disturbance, causing them to have higher uncertainties of ≥ ±0.000035. These values are slightly modified from those reported by Koffman et al. (2021b) and have been updated in the EarthChem database (Koffman et al., 2022). We digested and analyzed U.S. Geological Survey (USGS) rock standard BCR-2 to ensure accuracy of $^{87}Sr/^{86}Sr$ (0.705021 ± 0.000019, $n = 2$, 2$\sigma$) and $^{143}Nd/^{144}Nd$ (0.512647 ± 0.000021, $n = 6$, 2$\sigma$). Measurements are within the 2$\sigma$ error envelopes of the "preferred values" of

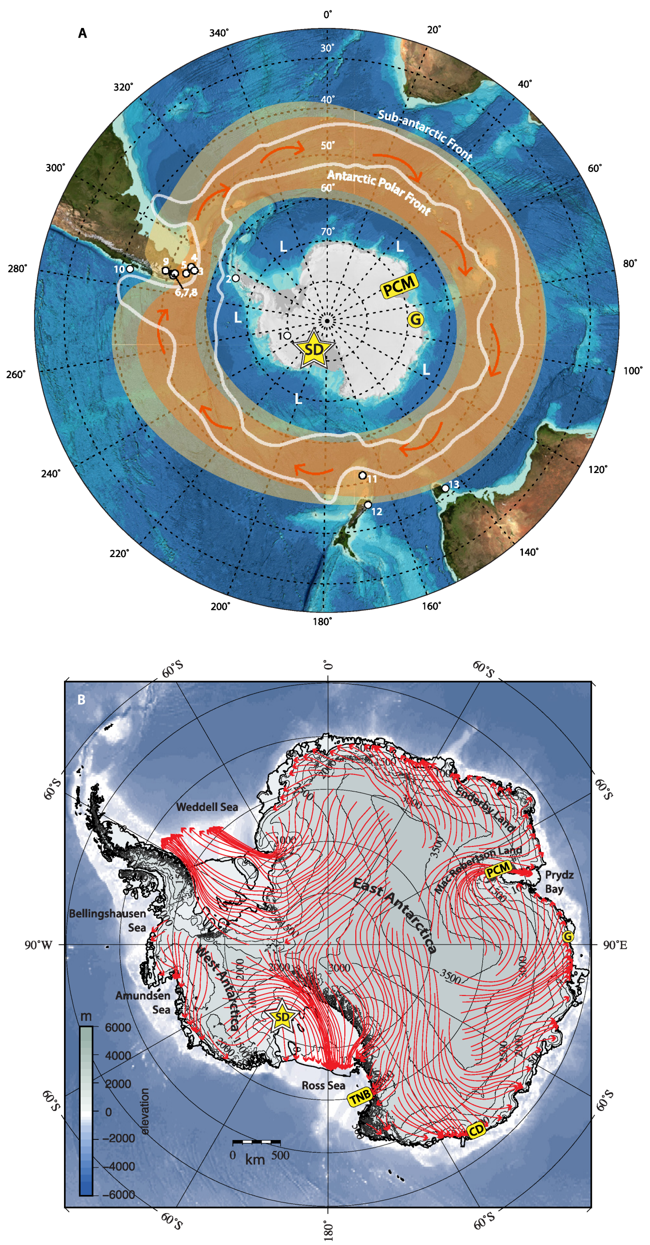


**Figure 1.** Overview maps highlighting (a) the modern Southern Hemisphere westerly wind belt (orange band), oceanic fronts, and region of atmospheric low pressure (depicted as Ls); (b) katabatic flow directions (red lines) based on Parish and Bromwich (2007). The channelized flow through the Prince Charles Mountains is of particular relevance for this study. Sites discussed in the text include: Siple Dome (SD), Gaussberg Volcano (G), Cape Denison (CD), Terra Nova Bay (TNB), and the Prince Charles Mountains (PCM). Numbered sites in (a) are: (1) WAIS Divide ice core, (2) Anvers Island, (3) Cordillera Darwin, (4) Ariel Peatland, (5) Marcelo Arévalo cave, (6) Lago Guanaco, (7) Lago Cipreses, (8) Torres del Paine, (9) Glaciar Torre, (10) Marine core GeoB 3313-1, (11) Auckland Islands, (12) Doubtful Sound, Fiordland, (13) Rebecca Lagoon, Tasmania.

Jweda et al. (2015), $^{87}Sr/^{86}Sr = 0.705000 \pm 0.000011$ and $^{143}Nd/^{144}Nd = 0.512637 \pm 0.000013$. Complete analytical details can be found in Koffman et al. (2021b).

REE concentrations of digested samples were measured on a VG PQ ExCell quadrupole ICP-MS at LDEO. We determined concentrations via standard additions at four dilutions spanning the expected concentrations of our samples. Instrumental drift was assessed by running a mixed-matrix standard every fifth sample. We analyzed USGS rock standard BCR-2 as a "random" sample to ensure accuracy of measurement (Jochum et al., 2016). We calculate the percent residual standard deviation (%RSD) using data from six independent digestions and seven independent analyses of BCR-2. We find %RSDs <8% for all elements except Co, As, Ag, and Cd, which are among the lowest-concentration elements for BCR-2 (Koffman et al., 2022). Because we were unable to weigh the ice core dust samples, we were unable to measure absolute concentrations. Instead, we report all REE relative to a Yb concentration consistent with our estimated mixture of end-members, which is Yb = 1.73 ppm. Complete details of REE analyses can be found in the Supporting Information of Koffman et al. (2021b).

The data are plotted on the most recent published timescale for Siple Dome (Taylor et al., 2004). The late Holocene portion of the timescale was developed using automated annual layer counting of electrical conductivity signals, with ages forced to be consistent with volcanic and beryllium-10 ($^{10}Be$) tie-points. The age uncertainty in the depth range of 0–230 m, which encompasses all our samples, is well-constrained by $^{10}Be$ tie-points and estimated at 5% (Taylor et al., 2004). Thus, absolute age uncertainties associated with our samples range from 9 to 14 yr during the LIA interval, and from 37 to 46 yr during the MCA interval. Although absolute ages carry this uncertainty, this is a floating chronology between tie-points, and the relative ages of the samples are much more precise. Each sample integrates about one decade worth of time.

## 3. Results and Discussion

### 3.1. Siple Dome Ice Core Dust Compositions

Considering Sr-Nd isotopes together, the Siple Dome samples show unique compositions compared to other Antarctic dust samples such as from Taylor Glacier, Talos Dome, Vostok, EPICA Dome C, and the McMurdo Dry Valleys (Koffman et al., 2021b). Although individually the $\varepsilon$Nd values overlap with other localities, as do the $^{87}Sr/^{86}Sr$ values, in combination they are unique, showing the lowest $^{87}Sr/^{86}Sr$ values (~0.7087–0.7102) among samples with comparable $\varepsilon$Nd values (−16.3 to −7.3). In a previous study, we used Sr-Nd isotopes, REEs, and Sm/Nd ratios to show that Siple Dome dust most likely comes from a mixture of three main sources: Patagonia in South America, Archean to early Proterozoic highly metamorphosed crust in East Antarctica, and either the Gaussberg lamproite or a source with a similar composition, also in East Antarctica (Figure 2; Koffman et al., 2021b). Other potential dust sources, whether in the midlatitudes or in Antarctica, generally have $\varepsilon$Nd or Sr isotope values that are too high to be compatible as end-members to Siple Dome (Figure 2). Mixing calculations for both Sr-Nd isotopes and REEs suggest, on the whole, roughly equal proportions of dust delivered to Siple Dome from coastal East Antarctica and Patagonia over our study interval (Koffman et al., 2021b).

10.1029/2022PA004543

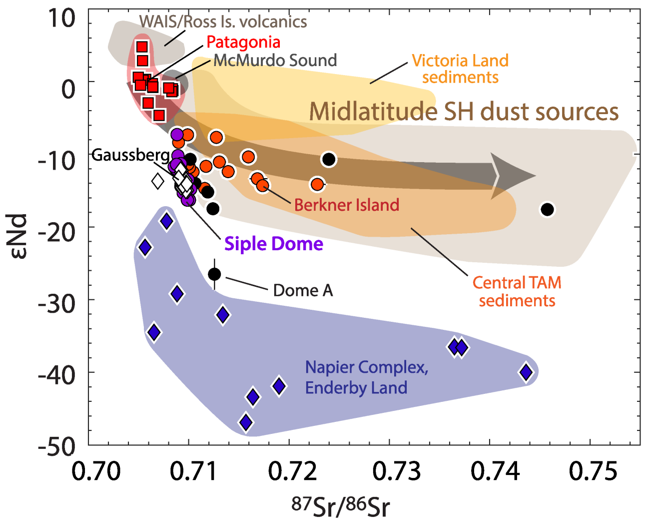


**Figure 2.** Comparison of Siple Dome $\varepsilon$Nd versus $^{87}Sr/^{86}Sr$ with recent snow measurements from Dome A and an associated transect (Du et al., 2018) and Berkner Island (Bory et al., 2010), along with potential source area data. Dome A and Berkner Island snow pit data cluster near Siple Dome, suggesting at least one shared dust source. Key sources thought to supply Siple Dome include Patagonia in South America (red squares), Gaussberg or material with a similar composition (white diamonds), and sediment derived from highly metamorphosed rocks (blue diamonds), both in East Antarctica. Most Southern Hemisphere (SH) midlatitude dust sources have either $\varepsilon$Nd or $^{87}Sr/^{86}Sr$ too high to be compatible as an end-member (beige outline and dark gray arrow). This is also true of sediments from Victoria Land (dark yellow) and the central Transantarctic Mountains (TAM, orange). Source area data citations: Blakowski et al. (2016), De Deckker (2019), Delmonte et al. (2004), DePaolo et al. (1982), Farmer and Licht (2016), Gili et al. (2017), Gingele and De Deckker (2005), Koffman et al. (2021a), McCulloch and Black (1984), Murphy et al. (2002), Panter et al. (2000, 1997), Revel-Rolland et al. (2006), Sims et al. (2008), Sims and Hart (2006), Sugden et al. (2009), Sushchevskaya et al. (2014), and Winton et al. (2016).

In the Sr and Nd isotope time series (Figure 3), lower $^{87}Sr/^{86}Sr$ covaries with higher $\varepsilon$Nd ($r = -0.72$), indicating that the mixing ratios of dust sources vary systematically. The MCA time series record (∼1030–1202 CE) shows two distinct intervals bounded at 1125 ± 41 CE. Over the first interval, ∼1030–1125 CE, $^{87}Sr/^{86}Sr$ values remain relatively stable at 0.7099 ± 0.0002 ($1\sigma$); and $\varepsilon$Nd ranges between ∼ −13 and −16. The data sets show a brief dip to lower Sr isotopes and higher $\varepsilon$Nd at 1087 ± 43 CE, with $\varepsilon$Nd reaching −12.9 at 1106 CE (discussed below). The most notable feature in the MCA record is an abrupt, sustained shift toward lower $^{87}Sr/^{86}Sr$ and higher $\varepsilon$Nd values at about 1125 ± 41 CE. The transition spans about two decades (e.g., 1115 CE to 1135 CE). Following the transition, $^{87}Sr/^{86}Sr$ values stay nearly constant (at 0.7088 ± 0.0001, $1\sigma$) for about 60 yr before returning to 0.7094 at 1202 ± 37 CE, while $\varepsilon$Nd values mainly vary between −11 and −13, with two notable brief positive excursions to −7.3 at 1125 ± 41 CE and −9.6 at 1195 ± 38 CE. In the LIA interval, ∼1665–1771 CE, Sr isotope values remain mainly between ∼0.7094 and 0.7095, with a shift to lower values of 0.7090 occurring between 1717 ± 12 CE and 1748 ± 10 CE and lasting for several decades. Sr values return to ∼0.7095 between ∼1756 and 1771 CE. $\varepsilon$Nd generally follows the same pattern as the Sr isotopes, with values mainly between ∼ −13 and −15, and also shows a positive shift between ∼1717 and ∼1748 CE, reaching $\varepsilon$Nd = −10.2 at ∼1756 CE and returning to −15.3 by ∼1771 CE.

Two possible explanations for the observed 60 yr change in dust composition occurring at ∼1125 CE and the shorter ∼20 yr shift occurring at ∼1748 CE are (a) a greater proportion of dust sourced from Patagonia, or (b) the sustained presence of tephra from regional volcanoes in the core. Antarctica and the subantarctic islands include multiple active volcanoes, and numerous eruptions have been detected in the Siple Dome ice core through statistical assessment of sulfate and other major ions (Kurbatov et al., 2006).

We are able to exclude tephra as the cause of the sustained, multi-decade shifts in Sr-Nd isotopes at ∼1125 CE and ∼1748 CE thanks to a detailed assessment of volcanic products in this ice core, which is on the same timescale used in this study. Eleven eruptions were detected during our MCA interval and three in our LIA interval on the basis of elevated sulfate concentrations (Figure 3f); however, not a single one of these sulfate peaks was accompanied by tephra grains in 0.2 μm filtered samples (Kurbatov et al., 2006). The search for tephra was systematic. Meltwater samples corresponding to each of the detected volcanic horizons were filtered and assessed using optical microscopy; if tephra was found, the samples were analyzed on an electron microprobe in order to determine the likely source volcanoes (Kurbatov et al., 2006). Because no tephra grains were found associated with any of the eruptions occurring during our study periods, we conclude it is unlikely that tephra deposition can explain the observed systematic multidecadal variability in the Sr-Nd time series. Moreover, episodic volcanic eruptions (typically lasting a year or less) would be unlikely to cause the decades-long variations in Sr-Nd isotope compositions observed in the Siple Dome record. We favor the first explanation, that the multidecadal shifts toward higher $\varepsilon$Nd – lower $^{87}Sr/^{86}Sr$ indicate a change in the continental dust source, specifically an increased proportion supplied by Patagonia.

While the Sr-Nd records generally show systematic variation, there are several relatively short-term superimposed positive $\varepsilon$Nd excursions that bear examination (Figure 3). These are characterized by significant shifts of ∼1.6–5 $\varepsilon$ units shown by individual samples, and occur at 1030 ± 46 CE ($\varepsilon$Nd = −13.5, $\Delta\varepsilon$Nd = 2.8, where $\Delta\varepsilon$Nd is defined as the difference between the excursion value and the average of the two points immediately before and after, if available), 1106 ± 42 CE ($\varepsilon$Nd = −12.9, $\Delta\varepsilon$Nd = 1.65), 1135 ± 41 CE ($\varepsilon$Nd = −7.3, $\Delta\varepsilon$Nd = 5.3), 1195 ± 38 CE ($\varepsilon$Nd = −9.6, $\Delta\varepsilon$Nd = 3.35), and 1677 ± 14 CE ($\varepsilon$Nd = −11.3, $\Delta\varepsilon$Nd = 2.55). We consider the first two $\varepsilon$Nd values, at 1030 and 1040 CE, to be related to the same event. The sample at 1756 ± 10 could be considered to have anomalously high $\varepsilon$Nd; however, this sample is part of a multidecadal shift seen in both Nd and Sr isotopes, and thus we do not consider it an excursion. Of the $\varepsilon$Nd excursions, unfortunately the ones at

10.1029/2022PA004543

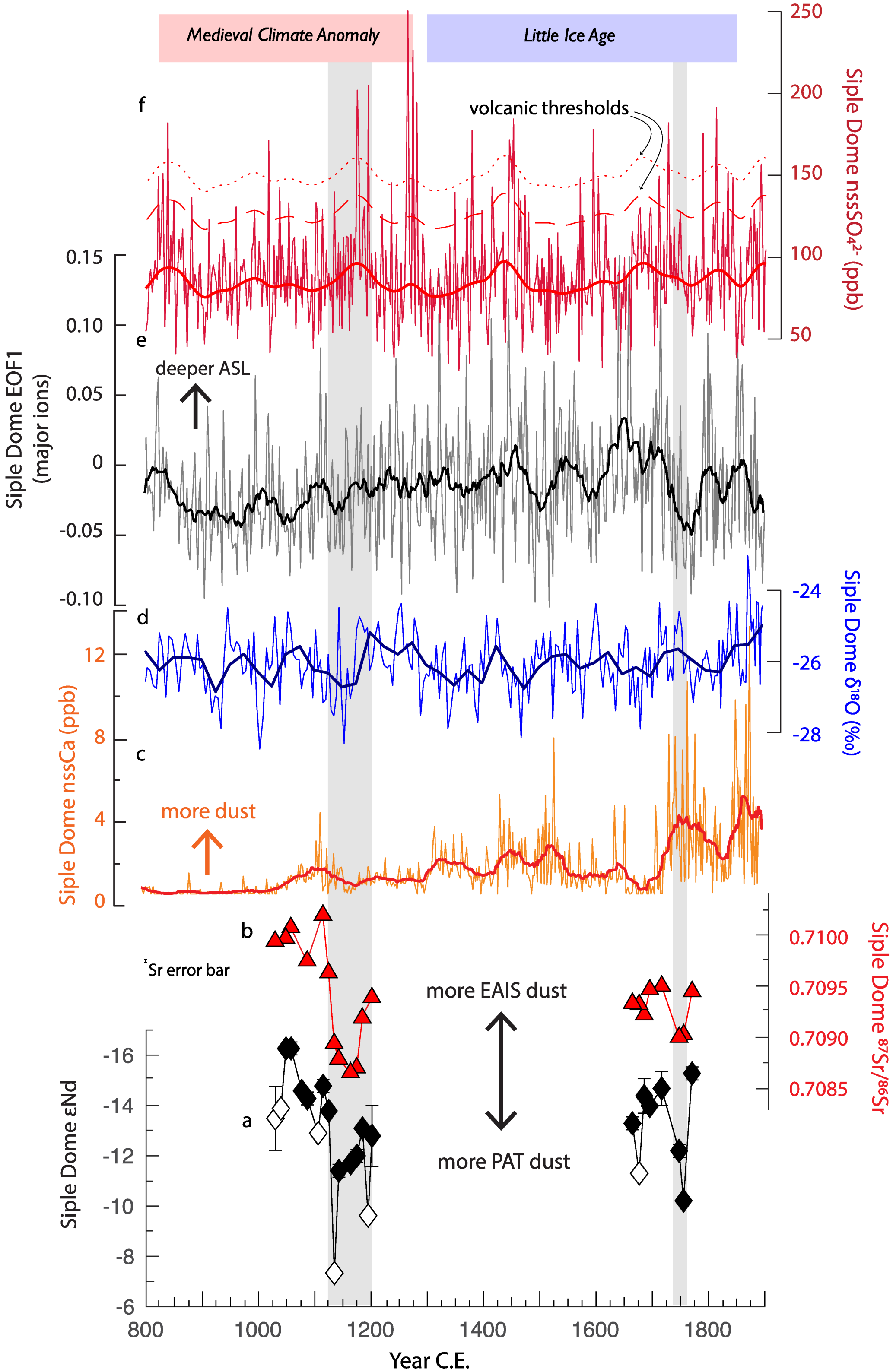


**Figure 3.**

~1106 CE and ~1195 CE do not have corresponding Sr isotope measurements. The other events at ~1030 CE, ~1135 CE, and ~1677 CE have Sr isotope values that follow the longer-term trends in the data; that is, they do not appear anomalous. In sum, we identify three $\varepsilon$Nd positive excursions in the record that consist of short-term (typically one sample) changes of ~1.6–5 $\varepsilon$ units and which are not paralleled by a major shift in Sr isotope values and two $\varepsilon$Nd positive excursions for which we do not have accompanying Sr isotope data. These excursions therefore appear to require input from a particle source affording Sr isotope values close to 0.708–0.709, consistent with the long-term trends, and by $\varepsilon$Nd values > −7 and likely much higher.

Although a change in the South American source regions supplying dust to Siple Dome could potentially account for these relatively brief positive $\varepsilon$Nd excursions (e.g., Patagonia and Tierra del Fuego display Sr isotope ratios of 0.705–0.712 and $\varepsilon$Nd of −5 to +6 [Gili et al., 2017]), a volcanic explanation in this case seems most plausible. We think these excursions may be caused by tephra because volcanic eruptions were identified at 1035 CE, 1100 CE, 1111 CE, 1132 CE, and 1193 CE on the basis of elevated sulfate concentrations (Figure 3), using the same timescale (Kurbatov et al., 2006). Although tephra horizons were not found for these eruptions, small grains would have been difficult to detect via optical microscopy, yet could have influenced the Sr-Nd isotope measurements given the low dust concentrations across this interval in our data (Figure 3). West Antarctic Rift System (WARS) volcanism would be the most likely volcanic source, given the number of active volcanoes within close proximity to Siple Dome, as evidenced by the predominance of tephra sourced from West Antarctic volcanoes in the Siple Dome core (Dunbar & Kurbatov, 2011). Eruptions occurring in the mid-latitudes, such as Cerro Hudson in Chile (1035 CE) are also plausible sources (Koffman et al., 2017; Kurbatov et al., 2006). While cryptotephra from more distal eruptions in the low latitudes has been documented in Antarctica (Koffman et al., 2013), grains tend to be small and sparse; thus we expect them to impart little influence on the isotope ratios, compared with mid-to-high latitude sources. Antarctic ice core data show that a substantial regional volcanic end-member must have Sr isotope ratios of ~0.708–0.709 coupled with $\varepsilon$Nd values of ~ +6 (Koffman et al., 2021a). A volcanic end-member composition of $\varepsilon$Nd ~ +6 and $^{87}$Sr/$^{86}$Sr ~ 0.708 would have a much greater impact on Siple Dome Nd isotope ratios than on Sr isotope ratios, which could explain the observed relatively brief $\varepsilon$Nd excursions that occur seemingly unaccompanied by Sr isotope excursions.

REE concentrations can help constrain potential source inputs to the samples showing $\varepsilon$Nd excursions. These samples tend to have slightly lower-than-average light REE (LREE) compared to other Siple Dome samples, though differences are not statistically significant (Figure S1 in Supporting Information S1). Because the REE patterns of Patagonian dust and WARS volcanics are very similar, with relatively low North American Shale Composite-normalized LREE, either of these sources could explain the tendency toward lower LREE in the excursion samples (Goldstein & Jacobsen, 1988; Wu et al., 2020). By comparison, EAIS metamorphic rocks have slightly higher LREE and much higher HREE (Liu et al., 2014). Thus, while REE are not able to discriminate between these two potential inputs to Siple Dome, they show that either source would be consistent with the observed $\varepsilon$Nd excursions (Figure S1 in Supporting Information S1).

Abundances of insoluble mineral dust particles have not, to our knowledge, been measured in the Siple Dome ice core. However, soluble nssCa (non-sea salt calcium) measured by ion chromatography can serve as a proxy for mineral dust in ice cores (Lambert et al., 2012; Ruth et al., 2008). The limitations of using soluble nssCa as a dust proxy are that it assumes a constant proportion of soluble Ca through time and cannot account for changes in mineralogy which might be indicated by a broader suite of insoluble elements as measured by inductively coupled plasma mass spectrometry (ICP-MS). In addition, soluble nssCa does not provide information on particle size distributions, which can serve as an independent proxy for past wind strength (Koffman et al., 2014) and may also affect elemental solubility (Baker & Jickells, 2006). Nonetheless, soluble nssCa is widely measured in ice core studies and provides valuable information about past dustiness when measures of insoluble dust are not available (e.g., Fuhrer et al., 1999; Lambert et al., 2012; Mayewski et al., 1994).

**Figure 3.** Siple Dome ice core climate records including: (a) $\varepsilon$Nd and (b) $^{87}$Sr/$^{86}$Sr isotope data, (c) non-sea salt Ca as a proxy for mineral dust (Mayewski et al., 2009), (d) $\delta^{18}$O as an indicator of past temperature (Steig & White, 2003), (e) a reconstruction of the Amundsen Sea Low (ASL) based on the first empirical orthogonal function (EOF1) of major ion data (Kreutz et al., 2000), and (f) non-sea-salt sulfate as an indicator of explosive volcanic eruptions (Kurbatov et al., 2006). Open symbols in (a) designate samples inferred to be influenced by tephra. Thick lines in (c and e) show 15-point running means. Thick line in (d) shows 25 yr resampled data. Thick red line in (f) uses a robust spline to estimate the background concentrations, and volcanic threshold values are based on the background plus the mean of all positive residuals, plus one standard deviation (dashed line) or two standard deviations (dotted line; Kurbatov et al., 2006). Brief positive $\varepsilon$Nd excursions can be seen at ~1106 CE, ~1135 CE, ~1195 CE, and ~1677 CE, which we attribute to the presence of small volcanic particles (see text). Sr error bars are smaller than symbols; a representative error bar is shown in panel (b).

10.1029/2022PA004543

Comparison of the Sr-Nd time series with the Siple Dome nssCa record (Figure 3c) shows that the ∼1125 CE change in the Sr-Nd isotopic composition was not accompanied by an increase in dust deposition. This means that the inferred increase in the proportion of dust supplied by Patagonia cannot be explained simply by greater dust emissions (i.e., source strength) or reduced washout during transport. Instead, the change in dust provenance at ∼1125 CE, indicated by Sr-Nd isotopes, occurs during a time of slightly decreasing nssCa concentrations. These observations imply a role for larger-scale atmospheric circulation changes. In this case, the data suggest a simultaneous decrease in the relative transport of dust from coastal EAIS sources and an increase in the relative transport of dust from Patagonia, resulting in an increase in the latter's contribution to Siple Dome. In contrast, the ∼1748 CE shift toward more Patagonia-like Sr-Nd compositions is accompanied by increased nssCa concentrations at Siple Dome (Figure 3), suggesting that higher dust emissions and/or reduced rainout of dust en route from Patagonia (cf. Markle et al., 2018) could explain the observed change in dust composition during the LIA interval.

### 3.2. Inferred Dust Transport Pathways

Dust from South American and East Antarctic source regions would necessarily follow different transport pathways to reach Siple Dome. Katabatic winds are associated with significant dust transport and aeolian landforms in glaciated regions around the world, including Antarctica (Bullard, 2013; Bullard et al., 2016). Persistent katabatic winds blowing off the EAIS would tend to entrain dust from East Antarctic sites including key coastal locations such as the Prince Charles Mountains in Mac Robertson Land (Figure 1b). Katabatic flow is highly nonuniform, and drainage is strongly controlled by topography and orientation (i.e., slope and aspect) of the ice sheet surface (Parish & Bromwich, 1987). This leads to regions of channelized katabatic drainage off the ice sheet, such as the well-studied locations of Terra Nova Bay in Victoria Land and Cape Denison in Adélie Land, known for the strongest sea-level winds on Earth (Figure 1b; Bromwich, 1989; Wendler et al., 1997). One of the largest such katabatic drainage systems flows through the steep terrain of coastal Mac Robertson Land and into Prydz Bay (Figure 1b; Parish & Bromwich, 1987, 1991, 2007). Upon reaching the ocean, katabatic winds decelerate and the air experiences significant rising motion from the coast to the mean circumpolar trough location at around 60°–65° (Parish & Bromwich, 2007). We expect that dust carried by katabatic winds would be incorporated into storms at these lower latitudes and deposited on the ice sheet with precipitation.

The katabatic wind convergence zone of Mac Robertson Land (Figure 1b) is of particular interest to this study, as bedrock that is geochemically compatible with the distinctive source rocks that supply the dust to Siple Dome with low $\varepsilon$Nd values and corresponding unusually low $^{87}Sr/^{86}Sr$, underlies the ice sheet in this region (Figure 2; Koffman et al., 2021b). This includes both Archean to early Proterozoic granulite-facies metamorphic rocks and recently erupted lamproites, such as Mt. Bayliss in the southern Prince Charles Mountains (Bergman, 1987). An obvious question is how can this region, far removed from Siple Dome, be a source of the Siple Dome dust? A possible mechanism is that glacial flour derived from these rocks is produced through ice-sheet erosion, deposited in the Prince Charles Mountains, and transported by the extreme, channelized katabatic winds in this region. Although other coastal EAIS locations such as Enderby Land and Gaussberg also contain source material geochemically compatible as the low $\varepsilon$Nd end-member to Siple Dome (Figure 1b; Koffman et al., 2021b), Mac Robertson Land is favored here because its wind regime strongly supports transport from sites within the Prince Charles Mountains (Parish & Bromwich, 1987, 2007). Given the similarities in Sr-Nd isotope compositions between Siple Dome, Dome A and an associated transect (Du et al., 2018), and Berkner Island (Bory et al., 2010; Figure 2), this region may supply dust to multiple sectors of Antarctica.

South American dust deposition in East Antarctica has been well-documented based on geochemical measurements from ice cores (Delmonte et al., 2008, 2004; Gili et al., 2016; Marino et al., 2009), and models suggest a predominant influence of South American dust in East Antarctica during both the Last Glacial Maximum and today (Albani et al., 2011; Li et al., 2008). Located in the midlatitudes, dust sources in Patagonia and Tierra del Fuego lie directly in the path of the SWW; modern dust emissions can be observed via satellite as dust travels eastward over the South Atlantic (Gassó & Stein, 2007; Gassó et al., 2010). In addition, South American dust sources to the north of Patagonia such as the Puna-Altiplano Plateau and Central Western Argentina may experience predominant northwesterly winds, carrying dust southeastward into the path of the SWW (Cosentino et al., 2020; Gaiero, 2007; Gaiero et al., 2013). Based on a combination of Sr-Nd isotopes and REE, Patagonia is inferred to be the higher $\varepsilon$Nd – lower $^{87}Sr/^{86}Sr$ end-member supplying dust to Siple Dome (Koffman et al., 2021b).

Changes in climate, including temperature, precipitation, and high-to-mid-latitude atmospheric pressure gradients, are likely to influence the relative proportions of dust reaching Siple Dome from such geographically and climatically distinct source regions as Patagonia and Mac Robertson Land. In the case of dust transport from Mac Robertson Land, the strength of the north-south pressure gradient directly enhances or inhibits gravity-driven flow off the ice sheet (Wendler et al., 1997). Deeper lows in the low-pressure trough near the coast (Figure 1) are associated with higher wind speeds, due to increased pressure gradient force, and because geostrophic winds reinforce the katabatic winds (Wendler et al., 1997). Colder temperatures are related to stronger temperature inversions and thus stronger katabatic force (Wendler et al., 1997). Overall, we would expect to see greater dust transport from coastal Mac Robertson Land during times with colder temperatures and more storms (i.e., below-average sea-level pressure). Conversely, dust transport from this region is expected to decrease during warmer climate intervals and periods with high sea-level pressure anomalies near the coast. This interpretation provides a testable hypothesis for future modeling efforts.

Because the main dust source regions of Patagonia and Tierra del Fuego lie in the direct path of the mid-latitude SWW band, we may expect that the relationship between winds and dust transport is fairly straightforward. At present, positive phases of the Southern Annular Mode (SAM+) are characterized by high SWW velocities and a southerly shift of the main wind belt. Transport of dust from Patagonia is likely to be enhanced during periods of dryness or increased SWW strength. Alternatively, the location of the wind belt also plays a role, and during periods of negative SAM, when the SWW extend farther north, there could be more dust emitted from northern dust sources (Neff & Bertler, 2015). A southward net SWW shift during Holocene warm periods such as the MCA interval, including in summer, may increase dust transport to Antarctica. In addition, on centennial to millennial timescales, changes in vegetation cover, aridity, and glacier activity are likely to play a role in local dust emissions (Fischer et al., 2007; Sugden et al., 2009). Wind gustiness, that is, the occurrence of high-speed wind events in dust source areas linked to steepened meridional temperature gradients, also likely plays a role in driving dust emissions (McGee et al., 2010). In the recent past, deforestation and agricultural land-use changes have also increased dust emissions from South American dust sources (McConnell et al., 2007). Regardless of the specific processes, our findings imply a role for Patagonia-Tierra del Fuego sources supplying dust to Siple Dome during the late Holocene.

### 3.3. Atmospheric Circulation During the Common Era

The Siple Dome Sr-Nd time series show an abrupt shift at 1125 ± 41 CE toward higher $\varepsilon$Nd-lower $^{87}$Sr/$^{86}$Sr (more Patagonia-like) values, which persist for about 60 yr (Figure 4). This change in dust composition coincides with a phase change from negative to strongly positive reconstructed SAM index values (Dätwyler et al., 2018) and corresponds with the beginning of a period of increased variability in coarse particle percentage in the WAIS Divide ice core, related to inferred poleward-shifted SWW (Koffman et al., 2014). The observed ~60 yr shift in Sr-Nd compositions coincides with a period of reduced ice extent on the Antarctic Peninsula (~65°S, Figure 1a) as evidenced by terrestrial organic material exposed by retreating glaciers dating to ~980–1250 CE (970–700 yr BP; Hall et al., 2010). Warmer temperatures during ~1080–1450 CE (900–500 yr BP) were also recorded by the ODP Site 1098 core (~65°S, Figure 1a) from Palmer Deep, near Anvers Island, reflecting increased influence of Circumpolar Deep Water likely driven by intensified SWW (Shevenell et al., 2011). Ice cores in the western Ross Sea and central West Antarctica also document warmer temperatures during the MCA interval (Bertler et al., 2011; Orsi et al., 2012).

Farther to the north in South America, hydroclimate reconstructions from areas influenced by the SWW can be used to reconstruct changes in wind strength, thereby allowing inference about latitudinal shifts. The SWW play a primary role in driving precipitation variability, particularly where they intersect north-south mountain ranges such as the Andes, causing orographic precipitation (Garreaud, 2007). This is evidenced by strong correlations between wind strength and precipitation amount on the western side of the Andes (Moreno et al., 2018). Lacustrine records and glacier chronologies from southwestern Patagonia (~48°–52°S, Figure 1a) document a period of relatively warm, dry conditions from ~1050 to 1300 CE (900–650 yr BP), consistent with inferred southward-shifted SWW during this time (García et al., 2020; Moreno et al., 2018, 2014; Moy et al., 2008; Reynhout et al., 2019). Specifically, the Lago Cipreses (51°S) *Nothofagus* arboreal pollen (LC NAP) record indicates a warm/dry interval from 864 to 1156 CE (1086–794 yr BP), termed "CC2" (Moreno et al., 2018, 2014), while the $\delta^{18}$O record of *Pisidium* bivalves from Lago Guanaco (51°52' S) indicates increased evaporation during 1050–1400 CE (900–550 yr BP). Although the intervals of warmth recorded by these lakes do not start and end precisely at the same time, they overlap, and the records likely document similar changes in climate. A stalagmite from Marcelo Arévalo cave at 53°S and near-coastal marine core GeoB 3313-1 at 41°S (Figure 1a) also indicate

10.1029/2022PA004543



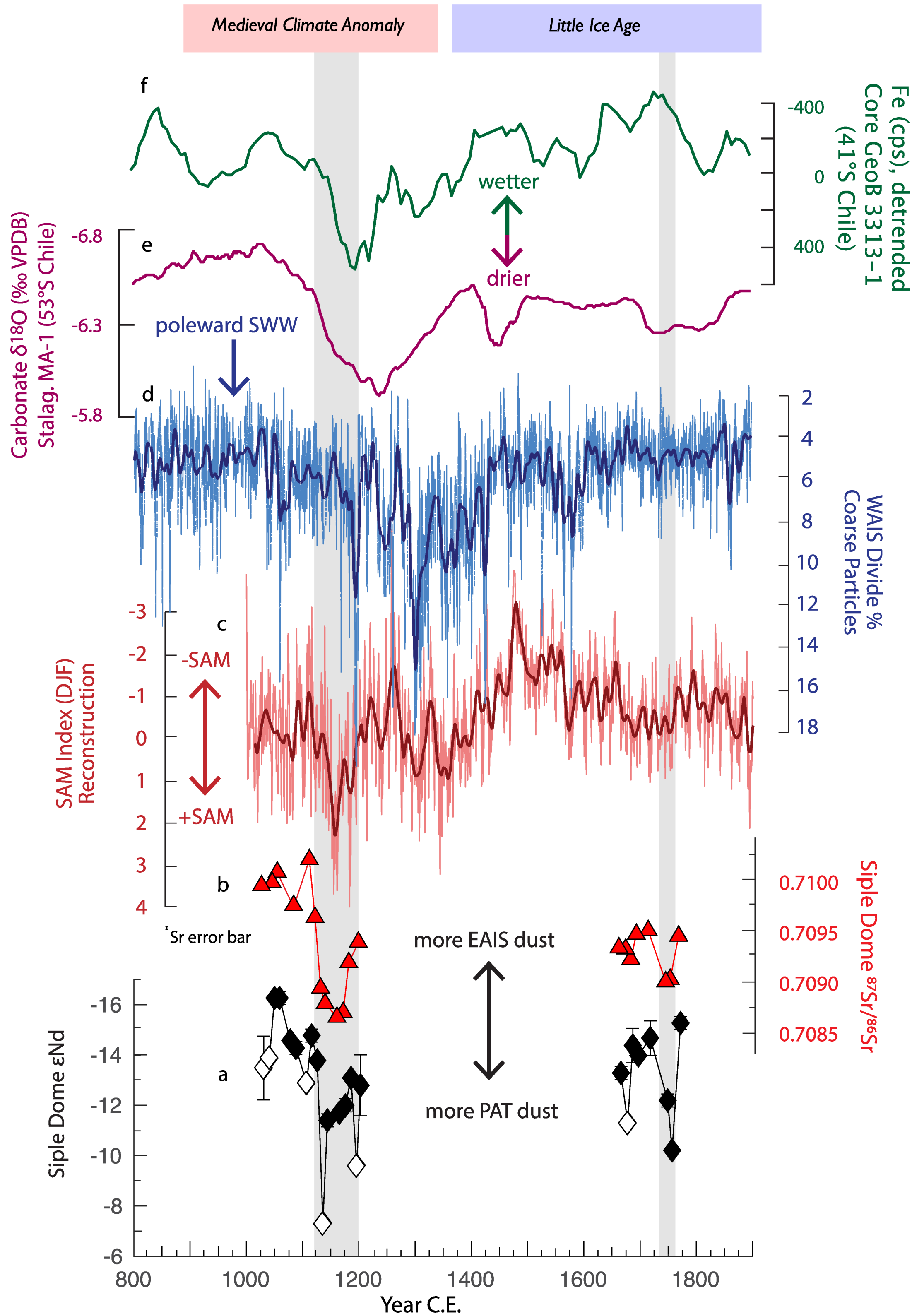


**Figure 4.**

10.1029/2022PA004543

a shift from wetter to drier conditions at ~1125 CE (Figure 4), consistent with weaker wind strength at these latitudes and a southward shift of the SWW belt. Given age uncertainties for all the records, it is difficult to ascertain whether these inferred changes were synchronous or sequential by latitude including their precise start and end date; however, the timing of changes in southwestern Patagonia appear to predate those seen at Siple Dome. If this is the case, it likely indicates that the SWW entered a phase of poleward contraction prior to the ~1125 CE shift documented by the Siple Dome Sr-Nd record.

In southernmost South America around the Tierra del Fuego - Cordillera Darwin region, paleoclimate records are also consistent with a southward shift of the SWW preceding or coinciding with the ~1125–1185 CE change in dust provenance observed at Siple Dome. An oxygen isotopic record of *Sphagnum* moss from Ariel Peatland (54°S, Figure 1a) indicates a period of stronger Andean rain shadow from 1020 to 1390 CE (930–560 yr BP), interpreted as stronger SWW at this latitude (Xia et al., 2018). Glaciers in Cordillera Darwin (~55°S), to the west, also may have responded to a southward shift in SWW at this time, which would have caused increased precipitation and reduced ablation; advances are dated to 1080 ± 60 CE (870 yr BP) and 1200 ± 110 CE (750 yr BP; Hall et al., 2019; Reynhout et al., 2022). Thus, while glaciers and hydroclimate reconstructions from farther north in Patagonia indicate warmer, drier conditions consistent with weakened SWW, records from 54° to 55°S perhaps are consistent with intensified SWW. Hence, together, records from the mid-latitudes of South America suggest that the Southern Hemisphere entered a period of generally SAM+ -like conditions with more zonally symmetric, poleward-shifted SWW by or before ~1125 CE, consistent with the Siple Dome record. The records indicate that this period of strong positive SAM-like conditions lasted about 60–100 yr (Figure 4), followed by a return to weakly SAM− conditions for ~100 yr (~1200–1300 CE; Dätwyler et al., 2018). This was followed by another ~100 yr of weak SAM+ conditions before a shift at ~1400 CE to more negative SAM index values, which prevailed throughout the LIA (Dätwyler et al., 2018).

In the western Pacific, land masses that intersect the northern margin of the SWW include the island of Tasmania in Australia and the South Island of New Zealand (NZ). Here, a marine sediment core from Doubtful Sound, Fiordland, NZ (45°S, Figure 1a) indicates a period of stronger SWW at 1125–1175 CE (825–775 yr BP), synchronous with the shift in Siple Dome dust provenance (Hinojosa et al., 2017). At ~1175 ± 35 CE, NZ fiord sediments document a weakening of the winds at this latitude, consistent with other records from the region (Hinojosa et al., 2017; Knudson et al., 2011). A lake sediment record from Rebecca Lagoon, Tasmania (41°S) also indicates wetter conditions during 950–1250 CE (1000–700 yr BP), overlapping the interval of stronger inferred SWW in Fiordland (Saunders et al., 2012). Intensification of the SWW during the MCA and weakening during the LIA is also suggested by a record from the Auckland Islands, in the core of the SWW belt at 51°40'S (Figure 1a) and south of the main islands of New Zealand (Browne et al., 2017). While the details of timing and latitude may differ somewhat between the New Zealand, Australian, and South American records, the overarching view is of zonally symmetric changes in the SWW during the past two millennia (Browne et al., 2017).

The highest positive preindustrial SAM index values (~3.56) of the past millennium (Dätwyler et al., 2018) occur right at the time when Siple Dome dust composition records its lowest $^{87}Sr/^{86}Sr$ and highest $\varepsilon$Nd values during the MCA interval (Figure 4), indicating the greatest relative input of dust from Patagonia. Considering the paleoenvironmental context surrounding this pulse of Patagonian dust (Figure 4), it seems likely that intensified SWW farther to the south facilitated higher dust emissions from southern portions of Patagonia and Tierra del Fuego into Antarctica. The rapidity of the shift in dust composition, occurring over a ~20 yr period, implicates an abrupt change in wind strength and/or positioning as the main driver of the observations. Concurrent with the increase in dust emissions from southern South America, we infer that warmer temperatures during the MCA in Antarctica likely diminished the strength of katabatic flow through the mountains of Mac Robertson Land, decreasing the transport of dust with an "older crustal" (lower $\varepsilon$Nd-higher $^{87}Sr/^{86}Sr$) isotopic composition to Siple Dome. This combination of increased dust emissions from southern Patagonia and reduced emissions from coastal EAIS is needed to explain the observed shift in Siple Dome dust isotopic composition, given that there was not a coincident increase in ice core dust concentration, as indicated by nssCa.

**Figure 4.** Comparison of Siple Dome $\varepsilon$Nd (a) and $^{87}Sr/^{86}Sr$ (b) isotope data with selected climate records from the Southern Hemisphere including (c) the DJF SAM reconstruction of Dätwyler et al. (2018) showing full resolution (lighter red) and 30 yr running mean (darker red) data, (d) the WAIS Divide ice core coarse particle percentage record showing 2 yr (lighter blue) and 10 yr (darker blue) running means (Koffman et al., 2014), (e) stalagmite MA-1 $\delta^{18}O$ (Schimpf et al., 2011), and (f) marine core GeoB3313-1 (Lamy et al., 2001). Open symbols in (a) designate samples inferred to be influenced by tephra. Together the records suggest that a rapid intensification of wind speed occurred at ~1125 CE during an interval of SAM+ -like conditions with generally poleward-shifted SWW. A shift in dust composition at ~1748 CE coincides with expanded glaciers in Patagonia and higher nssCa deposition at Siple Dome, likely indicating increased dust emissions related to glacier activity. Sr error bars are smaller than symbols; a representative error bar is shown in panel (b).

At ~1202 ± 37 CE, Siple Dome Sr isotopes increase and Nd isotopes decrease, reflecting a decrease in the relative contribution of Patagonian dust. This shift coincides with the onset of wetter and colder conditions in southwestern Patagonia (~48°–52°S), indicating stronger winds at these latitudes (Lamy et al., 2001; Moreno et al., 2018, 2014; Moy et al., 2008; Schimpf et al., 2011). A northward shift of the SWW belt at this time is indicated by a persistent trend toward negative SAM index values (Dätwyler et al., 2018; Figure 4). Consistent with this interpretation, following a period of relative warmth, glaciers in southern Patagonia (e.g., ~51°S, Figure 1a) experienced several advances associated with cooler and wetter conditions. Dating of moraines indicates these advances culminated around ~1350 CE (600 ± 70 yr BP), ~1420 CE (530 ± 60), ~1610 CE (340 ± 20 yr BP), and ~1760 CE (≤190 yr BP; García et al., 2020; Reynhout et al., 2019). Although the precise durations of these advances are uncertain, the cosmogenic exposure moraine ages likely reflect the latter part of a glacier expansion.

The second multidecade shift in Sr-Nd isotopes occurs at 1748 ± 10 CE. Unlike the shift at ~1125 CE, this change in dust composition is accompanied by a large peak in nssCa (Figure 3), indicating increased dust delivery to Siple Dome. Given expanded, erosive glaciers in Patagonia during this time (García et al., 2020; Reynhout et al., 2019), and the role of associated landscapes in generating fine-grained dust (Bullard, 2013; Prospero et al., 2012), we interpret this shift toward higher $\varepsilon$Nd – lower $^{87}$Sr/$^{86}$Sr values to reflect increased input of glaciogenic dust from southernmost South America (e.g., García et al., 2020), rather than just to a southward shift of the SWW. Further investigations can determine whether these decadal shifts in dust provenance are a recurrent feature associated with glacier expansion in Patagonia.

## 4. Conclusions

Sr-Nd isotope ratios measured in mineral dust from the Siple Dome ice core document a rapid one-to-two-decade shift in atmospheric circulation to the Ross Sea sector of Antarctica at ~1125 CE, which persists for about 60 yr. We infer a southward shift and strengthening of the SWW to explain the observed changes in dust transport to Siple Dome. The period from ~1125 to 1185 CE is superimposed on a multi-centennial interval characterized by positive SAM-like conditions with poleward-shifted or intensified SWW at more southern latitudes (~54°–55°S) and relatively warm, arid conditions farther north in southwestern Patagonia (~48°–52°S), corresponding approximately with the MCA period in the Northern Hemisphere. With the onset of cold conditions during the LIA interval, proxy records indicate a transition to negative SAM-like conditions with equatorward-shifted SWW and stronger winds along the northern margin of the wind belt. Siple Dome Sr-Nd isotopes during ~1665–1791 C.E reflect greater inputs of dust from coastal EAIS compared to the ~1125–1185 CE interval, consistent with cooler temperatures in Antarctica and stronger katabatic winds. This interval is punctuated by a ~20 yr shift in dust composition at ~1748 that may reflect increased glaciogenic dust emissions related to expanded, more erosive glaciers in South America. Finally, the data demonstrate that Sr-Nd isotopes can record shifts in atmospheric circulation on decadal timescales and suggest that additional high-resolution dust provenance records from ice cores show great potential for reconstructing past short-term and abrupt changes in wind belts.

## Conflict of Interest

The authors declare no conflicts of interest.

## Data Availability Statement

Siple Dome Sr-Nd and REE data are archived in the EarthChem Library (Koffman et al., 2022). Table S1 in Supporting Information S1 provides a summary of the isotope data used in this paper mapped to ages from Taylor et al. (2004).

**Acknowledgments**

This work was supported by NSF ANT 1204050 (Koffman) and ANT 1043471 (Kaplan, Goldstein, Winckler) and by an AAUW American Postdoctoral Research Leave Fellowship (Koffman). The authors appreciate Andrei Kurbatov, Karl Kreutz, Erich Osterberg, Aloys Bory, and Patricio Moreno for their helpful conversations. The authors thank Tom Williams and an anonymous reviewer for their thoughtful feedback, which served to clarify and strengthen the paper.

## References

Aarons, S., Aciego, S., McConnell, J., Delmonte, B., & Baccolo, G. (2019). Dust transport to the Taylor Glacier, Antarctica, during the last interglacial. *Geophysical Research Letters*, *46*(4), 2261–2270. https://doi.org/10.1029/2018gl081887

Albani, S., Mahowald, N. M., Delmonte, B., Maggi, V., & Winckler, G. (2011). Comparing modeled and observed changes in mineral dust transport and deposition to Antarctica between the Last Glacial Maximum and current climates. *Climate Dynamics*, *38*(9–10), 1731–1755. https://doi.org/10.1007/s00382-011-1139-5

Anderson, R. F., Ali, S., Bradtmiller, L. I., Nielsen, S. H. H., Fleisher, M. Q., Anderson, B. E., & Burckle, L. H. (2009). Wind-driven upwelling in the Southern Ocean and the deglacial rise in atmospheric $CO_2$. *Science*, *323*(5920), 1443–1448. https://doi.org/10.1126/science.1167441

Baker, A. R., & Jickells, T. D. (2006). Mineral particle size as a control on aerosol iron solubility. *Geophysical Research Letters*, *33*(17), L17608. https://doi.org/10.1029/2006gl026557

Bergman, S. C. (1987). Lamproites and other potassium-rich igneous rocks: A review of their occurrence, mineralogy, and geochemistry. *Geological Society, London, Special Publications*, *30*(1), 103–190. https://doi.org/10.1144/gsl.sp.1987.030.01.08

Bertler, N. A. N., Mayewski, P., & Carter, L. (2011). Cold conditions in Antarctica during the Little Ice Age—Implications for abrupt climate change mechanisms. *Earth and Planetary Science Letters*, *308*(1–2), 41–51. https://doi.org/10.1016/j.epsl.2011.05.021

Blakowski, M. A., Aciego, S. M., Delmonte, B., Baroni, C., Salvatore, M. C., & Sims, K. W. W. (2016). A Sr-Nd-Hf isotope characterization of dust source areas in Victoria Land and the McMurdo Sound sector of Antarctica. *Quaternary Science Reviews*, *141*, 26–37. https://doi.org/10.1016/j.quascirev.2016.03.023

Bory, A. J.-M., Biscaye, P. E., Svensson, A., & Grousset, F. (2002). Seasonal variability in the origin of recent atmospheric mineral dust at NorthGrIP, Greenland. *Earth and Planetary Science Letters*, *196*(3–4), 123–134. https://doi.org/10.1016/s0012-821x(01)00609-4

Bory, A. J.-M., Wolff, E., Mulvaney, R., Jagoutz, E., Wegner, A., Ruth, U., & Elderfield, H. (2010). Multiple sources supply eolian mineral dust to the Atlantic sector of coastal Antarctica: Evidence from recent snow layers at the top of Berkner Island ice sheet. *Earth and Planetary Science Letters*, *291*(1–4), 138–148. https://doi.org/10.1016/j.epsl.2010.01.006

Bromwich, D. H. (1989). An extraordinary katabatic wind regime at Terra Nova Bay, Antarctica. *Monthly Weather Review*, *117*(3), 688–695. https://doi.org/10.1175/1520-0493(1989)117<0688:aekwra>2.0.co;2

Browne, I. M., Moy, C. M., Riesselman, C. R., Neil, H. L., Curtin, L. G., Gorman, A. R., & Wilson, G. S. (2017). Late Holocene intensification of the westerly winds at the subantarctic Auckland Islands (51°S), New Zealand. *Climate of the Past*, *13*(10), 1301–1322. https://doi.org/10.5194/cp-13-1301-2017

Bullard, J. E. (2013). Contemporary glacigenic inputs to the dust cycle. *Earth Surface Processes and Landforms*, *38*(1), 71–89. https://doi.org/10.1002/esp.3315

Bullard, J. E., Baddock, M., Bradwell, T., Crusius, J., Darlington, E., Gaiero, D., et al. (2016). High-latitude dust in the Earth system. *Reviews of Geophysics*, *54*(2), 447–485. https://doi.org/10.1002/2016rg000518

Burke, A., & Robinson, L. F. (2012). The Southern Ocean's role in carbon exchange during the last deglaciation. *Science*, *335*(6068), 557–561. https://doi.org/10.1126/science.1208163

Cosentino, N. J., Gaiero, D. M., Torre, G., Pasquini, A. I., Coppo, R., Arce, J. M., & Vélez, G. (2020). Atmospheric dust dynamics in southern South America: A 14 yr modern dust record in the loessic Pampean region. *The Holocene*, *30*(4), 575–588. https://doi.org/10.1177/0959683619875198

Dätwyler, C., Neukom, R., Abram, N. J., Gallant, A. J., Grosjean, M., Jacques-Coper, M., et al. (2018). Teleconnection stationarity, variability, and trends of the Southern Annular Mode (SAM) during the last millennium. *Climate Dynamics*, *51*(5), 2321–2339. https://doi.org/10.1007/s00382-017-4015-0

De Deckker, P. (2019). An evaluation of Australia as a major source of dust. *Earth-Science Reviews*, *194*, 536–567. https://doi.org/10.1016/j.earscirev.2019.01.008

Delmonte, B., Andersson, P. S., Hansson, M., Schoberg, H., Petit, J. R., Basile-Doelsch, I., & Maggi, V. (2008). Aeolian dust in East Antarctica (EPICA-Dome C and Vostok): Provenance during glacial ages of the last 800 kyr. *Geophysical Research Letters*, *35*(7), L07703. https://doi.org/10.1029/2008GL033382

Delmonte, B., Basile-Doelsch, I., Petit, J. R., Maggi, V., Revel-Rolland, M., Michard, A., et al. (2004). Comparing the Epica and Vostok dust records during the last 220,000 yr: Stratigraphical correlation and provenance in glacial periods. *Earth-Science Reviews*, *66*(1–2), 63–87. https://doi.org/10.1016/j.earscirev.2003.10.004

Delmonte, B., Winton, H., Baroni, M., Baccolo, G., Hansson, M., Andersson, P., et al. (2020). Holocene dust in East Antarctica: Provenance and variability in time and space. *The Holocene*, *30*(4), 546–558. https://doi.org/10.1177/0959683619875188

Denton, G. H., Putnam, A. E., Russell, J. L., Barrell, D. J., Schaefer, J. M., Kaplan, M. R., & Strand, P. D. (2021). The Zealandia Switch: Ice age climate shifts viewed from Southern Hemisphere moraines. *Quaternary Science Reviews*, *257*, 106771. https://doi.org/10.1016/j.quascirev.2020.106771

DePaolo, D., Manton, W., Grew, E., & Halpern, M. (1982). Sm-Nd, Rb-Sr and U-Th-Pb systematics of granulite facies rocks from Fyfe Hills, Enderby Land, Antarctica. *Nature*, *298*(5875), 614–618. https://doi.org/10.1038/298614a0

Du, Z., Xiao, C., Ding, M., & Li, C. (2018). Identification of multiple natural and anthropogenic sources of dust in snow from Zhongshan Station to Dome A, East Antarctica. *Journal of Glaciology*, *64*(248), 855–865. https://doi.org/10.1017/jog.2018.72

Dunbar, N. W., & Kurbatov, A. V. (2011). Tephrochronology of the Siple Dome ice core, West Antarctica: Correlations and sources. *Quaternary Science Reviews*, *30*(13–14), 1602–1614. https://doi.org/10.1016/j.quascirev.2011.03.015

Farmer, G. L., & Licht, K. J. (2016). Generation and fate of glacial sediments in the central Transantarctic Mountains based on radiogenic isotopes and implications for reconstructing past ice dynamics. *Quaternary Science Reviews*, *150*, 98–109. https://doi.org/10.1016/j.quascirev.2016.08.002

Fischer, H., Fundel, F., Ruth, U., Twarloh, B., Wegner, A., Udisti, R., et al. (2007). Reconstruction of millennial changes in dust emission, transport, and regional sea ice coverage using the deep EPICA ice cores from the Atlantic and Indian Ocean sector of Antarctica. *Earth and Planetary Science Letters*, *260*(1–2), 340–334. https://doi.org/10.1016/j.epsl.2007.06.014

Fuhrer, K., Wolff, E. W., & Johnsen, S. J. (1999). Timescales for dust variability in the Greenland Ice Core Project (GRIP) ice core in the last 100,000 yr. *Journal of Geophysical Research: Atmospheres*, *104*(D24), 31043–31052. https://doi.org/10.1029/1999jd900929

Gaiero, D. M. (2007). Dust provenance in Antarctic ice during glacial periods: From where in southern South America? *Geophysical Research Letters*, *34*(17), L17707. https://doi.org/10.1029/2007gl030520

Gaiero, D. M., Simonella, L., Gassó, S., Gili, S., Stein, A., Sosa, P., et al. (2013). Ground/satellite observations and atmospheric modeling of dust storms originating in the high Puna-Altiplano deserts (South America): Implications for the interpretation of paleo-climatic archives. *Journal of Geophysical Research: Atmospheres*, *118*(9), 3817–3831. https://doi.org/10.1002/jgrd.50036

García, J.-L., Hall, B. L., Kaplan, M. R., Gómez, G. A., De Pol-Holz, R., García, V. J., et al. (2020). $^{14}C$ and $^{10}Be$ dated Late Holocene fluctuations of Patagonian glaciers in Torres del Paine (Chile, 51°S) and connections to Antarctic climate change. *Quaternary Science Reviews*, *246*, 106541. https://doi.org/10.1016/j.quascirev.2020.106541

Garreaud, R. (2007). Precipitation and circulation covariability in the extratropics. *Journal of Climate*, *20*(18), 4789–4797. https://doi.org/10.1175/jcli4257.1

Gassó, S., & Stein, A. F. (2007). Does dust from Patagonia reach the sub-Antarctic Atlantic Ocean? *Geophysical Research Letters*, *34*(1), L01801. https://doi.org/10.1029/2006gl027693

Gassó, S., Stein, A. F., Marino, F., Castellano, E., Udisti, R., & Ceratto, J. (2010). A combined observational and modeling approach to study modern dust transport from the Patagonia desert to East Antarctica. *Atmospheric Chemistry and Physics*, *10*(17), 8287–8303. https://doi.org/10.5194/acp-10-8287-2010

Gili, S., Gaiero, D. M., Goldstein, S. L., Chemale, F., Jr., Jweda, J., Kaplan, M. R., et al. (2017). Glacial/interglacial changes of Southern Hemisphere wind circulation from the geochemistry of South American dust. *Earth and Planetary Science Letters*, *469*, 98–109. https://doi.org/10.1016/j.epsl.2017.04.007

Gili, S., Gaiero, D. M., Goldstein, S. L., Chemale, F., Jr., Koester, E., Jweda, J., et al. (2016). Provenance of dust to Antarctica: A lead isotopic perspective. *Geophysical Research Letters*, *43*(5), 2291–2298. https://doi.org/10.1002/2016GL068244

Gingele, F. X., & De Deckker, P. (2005). Clay mineral, geochemical and Sr-Nd isotopic fingerprinting of sediments in the Murray-Darling fluvial system, southeast Australia. *Australian Journal of Earth Sciences*, *52*(6), 965–974. https://doi.org/10.1080/08120090500302301

Goldstein, S. J., & Jacobsen, S. B. (1988). Nd and Sr isotopic systematics of river water suspended material: Implications for crustal evolution. *Earth and Planetary Science Letters*, *87*(3), 249–265. https://doi.org/10.1016/0012-821x(88)90013-1

Grousset, F. E., & Biscaye, P. E. (2005). Tracing dust sources and transport patterns using Sr, Nd, and Pb isotopes. *Chemical Geology*, *222*(3–4), 149–167. https://doi.org/10.1016/j.chemgeo.2005.05.006

Hall, B. L., Koffman, T., & Denton, G. H. (2010). Reduced ice extent on the western Antarctic Peninsula at 700–970 cal. yr BP. *Geology*, *38*(7), 635–638. https://doi.org/10.1130/G30932.1

Hall, B. L., Lowell, T., Bromley, G., Denton, G., & Putnam, A. (2019). Holocene glacier fluctuations on the northern flank of Cordillera Darwin, southernmost South America. *Quaternary Science Reviews*, *222*, 105904. https://doi.org/10.1016/j.quascirev.2019.105904

Hinojosa, J. L., Moy, C. M., Stirling, C. H., Wilson, G. S., & Eglinton, T. I. (2017). A New Zealand perspective on centennial-scale Southern Hemisphere westerly wind shifts during the last two millennia. *Quaternary Science Reviews*, *172*, 32–43. https://doi.org/10.1016/j.quascirev.2017.07.016

Jochum, K. P., Weis, U., Schwager, B., Stoll, B., Wilson, S. A., Haug, G. H., et al. (2016). Reference values following ISO guidelines for frequently requested rock reference materials. *Geostandards and Geoanalytical Research*, *40*(3), 333–350. https://doi.org/10.1111/j.1751-908x.2015.00392.x

Jweda, J., Bolge, L., Class, C., & Goldstein, S. L. (2015). High precision Sr-Nd-Hf-Pb isotopic compositions of USGS reference material BCR-2. *Geostandards and Geoanalytical Research*, *40*(1), 101–115. https://doi.org/10.1111/j.1751-908X.2015.00342.x

Knudson, K. P., Hendy, I. L., & Neil, H. L. (2011). Re-examining Southern Hemisphere westerly wind behavior: Insights from a late Holocene precipitation reconstruction using New Zealand fjord sediments. *Quaternary Science Reviews*, *30*(21–22), 3124–3138. https://doi.org/10.1016/j.quascirev.2011.07.017

Koffman, B. G., Dowd, E. G., Osterberg, E. C., Ferris, D. G., Hartman, L. H., Wheatley, S. D., et al. (2017). Rapid transport of ash and sulfate from the 2011 Puyehue-Cordón Caulle (Chile) eruption to West Antarctica. *Journal of Geophysical Research: Atmospheres*, *122*(16), 8908–8920. https://doi.org/10.1002/2017JD026893

Koffman, B. G., Goldstein, S. L., Winckler, G., Kaplan, M. R., Bolge, L., Cai, Y., et al. (2021a). New Zealand as a source of mineral dust to the atmosphere and ocean. *Quaternary Science Reviews*, *251*(106659), 106659. https://doi.org/10.1016/j.quascirev.2020.106659

Koffman, B. G., Goldstein, S. L., Winckler, G., Kaplan, M. R., Kreutz, K. J., Bolge, L., et al. (2021b). Late Holocene dust provenance at Siple Dome, Antarctica. *Quaternary Science Reviews*, *274*, 107271. https://doi.org/10.1016/j.quascirev.2021.107271

Koffman, B. G., Goldstein, S. L., Winckler, G., Kaplan, M. R., Kreutz, K. J., Bolge, L., et al. (2022). Late Holocene Sr-Nd isotope and REE data from the Siple Dome ice core, Antarctica, Version 1.0. [Dataset]. Interdisciplinary Earth Data Alliance (IEDA). https://doi.org/10.26022/IEDA/112176

Koffman, B. G., Kreutz, K. J., Breton, D. J., Kane, E. J., Winski, D. A., Birkel, S. D., et al. (2014). Centennial-scale variability of the Southern Hemisphere westerly wind belt in the eastern Pacific over the past two millennia. *Climate of the Past*, *10*(3), 1125–1144. https://doi.org/10.5194/cp-10-1125-2014

Koffman, B. G., Kreutz, K. J., Kurbatov, A. V., & Dunbar, N. W. (2013). Impact of known local and tropical volcanic eruptions of the past millennium on the WAIS Divide microparticle record. *Geophysical Research Letters*, *40*(17), 4712–4716. https://doi.org/10.1002/grl.50822

Kreutz, K. J., Mayewski, P. A., Pittalwala, I. I., Meeker, L. D., Twickler, M. S., & Whitlow, S. I. (2000). Sea level pressure variability in the Amundsen Sea region inferred from a West Antarctic glaciochemical record. *Journal of Geophysical Research*, *105*(D3), 4047–4059. https://doi.org/10.1029/1999jd901069

Kurbatov, A. V., Zielinski, G. A., Dunbar, N. W., Mayewski, P. A., Meyerson, E. A., Sneed, S. B., & Taylor, K. C. (2006). A 12,000 yr record of explosive volcanism in the Siple Dome ice core, West Antarctica. *Journal of Geophysical Research*, *111*(D12307), D12307. https://doi.org/10.1029/2005JD006072

Lambert, F., Bigler, M., Steffensen, J. P., Hutterli, M. A., & Fischer, H. (2012). Centennial mineral dust variability in high-resolution ice core data from Dome C, Antarctica. *Climate of the Past*, *8*(2), 609–623. https://doi.org/10.5194/cp-8-609-2012

Lamy, F., Hebbeln, D., Rohl, U., & Wefer, G. (2001). Holocene rainfall variability in southern Chile: A marine record of latitudinal shifts of the southern westerlies. *Earth and Planetary Science Letters*, *185*(3–4), 369–382. https://doi.org/10.1016/s0012-821x(00)00381-2

Li, F., Ginoux, P., & Ramaswamy, V. (2008). Distribution, transport, and deposition of mineral dust in the Southern Ocean and Antarctica: Contribution of major sources. *Journal of Geophysical Research*, *113*(D10207), D10207. https://doi.org/10.1029/2007JD009190

Liu, X., Wang, W., Zhao, Y., Liu, J., & Song, B. (2014). Early Neoproterozoic granulite facies metamorphism of mafic dykes from the Vestfold Block, east Antarctica. *Journal of Metamorphic Geology*, *32*(9), 1041–1062. https://doi.org/10.1111/jmg.12106

Marcott, S. A., Bauska, T. K., Buizert, C., Steig, E. J., Rosen, J. L., Cuffey, K. M., et al. (2014). Centennial-scale changes in the global carbon cycle during the last deglaciation. *Nature*, *514*(7524), 616–619. https://doi.org/10.1038/nature13799

Marino, F., Castellano, E., Nava, S., Chiari, M., Ruth, U., Wegner, A., et al. (2009). Coherent composition of glacial dust on opposite sides of the East Antarctic Plateau inferred from the deep EPICA ice cores. *Geophysical Research Letters*, *36*(L23703), L23703. https://doi.org/10.1029/2009GL040732

Markle, B. R., Steig, E. J., Roe, G. H., Winckler, G., & McConnell, J. R. (2018). Concomitant variability in high-latitude aerosols, water isotopes, and the hydrologic cycle. *Nature Geoscience*, *11*(11), 853–859. https://doi.org/10.1038/s41561-018-0210-9

Mayewski, P. A., Meeker, L. D., Whitlow, S. I., Twickler, M. S., Morrison, M. C., Grootes, P. M., et al. (1994). Changes in atmospheric circulation and ocean ice cover over the North Atlantic during the last 41,000 yr. *Science*, *263*(5154), 1747–1751. https://doi.org/10.1126/science.263.5154.1747

Mayewski, P. A., Meredith, M. P., Summerhayes, C. P., Turner, J., Worby, A., Barrett, P. J., et al. (2009). State of the Antarctic and Southern Ocean climate system. *Reviews of Geophysics*, *47*(1), RG1003. https://doi.org/10.1029/2007rg000231

McConnell, J. R., Aristarain, A. J., Banta, J. R., Edwards, P. R., & Simoes, J. C. (2007). Twentieth -century doubling in dust archived in an Antarctic Peninsula ice core parallels climate change and desertification in South America. *Proceedings of the National Academy of Sciences of the United States of America*, *104*(14), 5743–5748. https://doi.org/10.1073/pnas.0607657104

McCulloch, M. T., & Black, L. P. (1984). Sm-Nd isotopic systematics of Enderby Land granulites and evidence for the redistribution of Sm and Nd during metamorphism. *Earth and Planetary Science Letters*, *71*(1), 46–58. https://doi.org/10.1016/0012-821x(84)90051-7

McGee, D., Broecker, W. S., & Winckler, G. (2010). Gustiness: The driver of glacial dustiness? *Quaternary Science Reviews*, *29*(17–18), 2340–2350. https://doi.org/10.1016/j.quascirev.2010.06.009

Moreno, P. I., Vilanova, I., Villa-Martínez, R., Dunbar, R., Mucciarone, D., Kaplan, M., et al. (2018). Onset and evolution of southern annular mode-like changes at centennial timescale. *Scientific Reports*, *8*(1), 1–9. https://doi.org/10.1038/s41598-018-21836-6

Moreno, P. I., Vilanova, I., Villa-Martínez, R., Garreaud, R., Rojas, M., & Pol-Holz, D. (2014). Southern Annular Mode-like changes in southwestern Patagonia at centennial timescales over the last three millennia. *Nature Communications*, *5*(1), 1–7. https://doi.org/10.1038/ncomms5375

Moy, C. M., Dunbar, R. B., Moreno, P. I., Francois, J.-P., Villa-Martinez, R., Mucciarone, D. M., et al. (2008). Isotopic evidence for hydrologic change related to the westerlies in SW Patagonia, Chile, during the last millennium. *Quaternary Science Reviews*, *27*(13–14), 1335–1349. https://doi.org/10.1016/j.quascirev.2008.03.006

Murphy, D., Collerson, K., & Kamber, B. (2002). Lamproites from Gaussberg, Antarctica: Possible transition zone melts of Archaean subducted sediments. *Journal of Petrology*, *43*(6), 981–1001. https://doi.org/10.1093/petrology/43.6.981

Neff, P. D., & Bertler, N. A. N. (2015). Trajectory modeling of modern dust transport to the Southern Ocean and Antarctica. *Journal of Geophysical Research: Atmospheres*, *120*(18), 9303–9322. https://doi.org/10.1002/2015JD023304

Orsi, A. J., Cornuelle, B. D., & Severinghaus, J. P. (2012). Little Ice Age cold interval in West Antarctica: Evidence from borehole temperature at the West Antarctic Ice Sheet (WAIS) Divide. *Geophysical Research Letters*, *39*(9), L09710. https://doi.org/10.1029/2012GL051260

Panter, K. S., Hart, S. R., Kyle, P., Blusztanjn, J., & Wilch, T. (2000). Geochemistry of Late Cenozoic basalts from the Crary Mountains: Characterization of mantle sources in Marie Byrd Land, Antarctica. *Chemical Geology*, *165*(3–4), 215–241. https://doi.org/10.1016/s0009-2541(99)00171-0

Panter, K. S., Kyle, P. R., & Smellie, J. L. (1997). Petrogenesis of a phonolite-trachyte succession at Mount Sidley, Marie Byrd Land, Antarctica. *Journal of Petrology*, *38*(9), 1225–1253. https://doi.org/10.1093/petroj/38.9.1225

Parish, T. R., & Bromwich, D. H. (1987). The surface wind field over the Antarctic ice sheets. *Nature*, *328*(6125), 51–54. https://doi.org/10.1038/328742b0

Parish, T. R., & Bromwich, D. H. (1991). Continental-scale simulation of the Antarctic katabatic wind regime. *Journal of Climate*, *4*(2), 135–146. https://doi.org/10.1175/1520-0442(1991)004<0135:cssota>2.0.co;2

Parish, T. R., & Bromwich, D. H. (2007). Reexamination of the near-surface airflow over the Antarctic continent and implications on atmospheric circulations at high southern latitudes. *Monthly Weather Review*, *135*(5), 1961–1973. https://doi.org/10.1175/mwr3374.1

Prospero, J. M., Bullard, J. E., & Hodgkins, R. (2012). High-latitude dust over the North Atlantic: Inputs from Icelandic proglacial dust storms. *Science*, *335*(1078), 1078–1082. https://doi.org/10.1126/science.1217447

Revel-Rolland, M., De Deckker, P., Delmonte, B., Hesse, P. P., Magee, J. W., Basile-Doelsch, I., et al. (2006). Eastern Australia: A possible source of dust in East Antarctica interglacial ice. *Earth and Planetary Science Letters*, *249*(1–2), 1–13. https://doi.org/10.1016/j.epsl.2006.06.028

Reynhout, S. A., Kaplan, M. R., Sagredo, E. A., Aravena, J. C., Soteres, R. L., Schwartz, R., & Schaefer, J. M. (2022). Holocene glacier history of northeastern Cordillera Darwin, southernmost South America (55°S). *Quaternary Research*, *105*, 166–181. https://doi.org/10.1017/qua.2021.45

Reynhout, S. A., Sagredo, E. A., Kaplan, M. R., Aravena, J. C., Martini, M. A., Moreno, P. I., et al. (2019). Holocene glacier fluctuations in Patagonia are modulated by summer insolation intensity and paced by Southern Annular Mode-like variability. *Quaternary Science Reviews*, *220*, 178–187. https://doi.org/10.1016/j.quascirev.2019.05.029

Rhodes, R., Bertler, N., Baker, J., Steen-Larsen, H., Sneed, S., Morgenstern, U., & Johnsen, S. (2012). Little Ice Age climate and oceanic conditions of the Ross Sea, Antarctica from a coastal ice core record. *Climate of the Past*, *8*(4), 1223–1238. https://doi.org/10.5194/cp-8-1223-2012

Ruth, U., Barbante, C., Bigler, M., Delmonte, B., Fischer, H., Gabrielli, P., et al. (2008). Proxies and measurement techniques in Antarctic Ice Cores. *Environmental Science & Technology*, *42*(15), 5675–5681. https://doi.org/10.1021/es703078z

Saunders, K. M., Kamenik, C., Hodgson, D. A., Hunziker, S., Siffert, L., Fischer, D., et al. (2012). Late Holocene changes in precipitation in northwest Tasmania and their potential links to shifts in the Southern Hemisphere westerly winds. *Global and Planetary Change*, *92*, 82–91. https://doi.org/10.1016/j.gloplacha.2012.04.005

Saunders, K. M., Roberts, S. J., Perren, B., Butz, C., Sime, L., Davies, S., et al. (2018). Holocene dynamics of the Southern Hemisphere westerly winds and possible links to $CO_2$ outgassing. *Nature Geoscience*, *11*(9), 650–655. https://doi.org/10.1038/s41561-018-0186-5

Schimpf, D., Kilian, R., Kronz, A., Simon, K., Spötl, C., Wörner, G., et al. (2011). The significance of chemical, isotopic, and detrital components in three coeval stalagmites from the superhumid southernmost Andes (53°S) as high-resolution palaeo-climate proxies. *Quaternary Science Reviews*, *30*(3–4), 443–459. https://doi.org/10.1016/j.quascirev.2010.12.006

Shevenell, A. E., Ingalls, A. E., Domack, E. W., & Kelly, C. (2011). Holocene Southern Ocean surface temperature variability west of the Antarctic Peninsula. *Nature*, *470*(7333), 250–254. https://doi.org/10.1038/nature09751

Sims, K. W., Blichert-Toft, J., Kyle, P. R., Pichat, S., Gauthier, P.-J., Blusztajn, J., et al. (2008). A Sr, Nd, Hf, and Pb isotope perspective on the genesis and long-term evolution of alkaline magmas from Erebus volcano, Antarctica. *Journal of Volcanology and Geothermal Research*, *177*(3), 606–618. https://doi.org/10.1016/j.jvolgeores.2007.08.006

Sims, K. W., & Hart, S. (2006). Comparison of Th, Sr, Nd, and Pb isotopes in oceanic basalts: Implications for mantle heterogeneity and magma genesis. *Earth and Planetary Science Letters*, *245*(3–4), 743–761. https://doi.org/10.1016/j.epsl.2006.02.030

Steig, E. J., & White, J. (2003). Siple Dome highlights: Stable isotopes, version 1.0 [Dataset]. U.S. Antarctic Program (USAP) Data Center. https://doi.org/10.7265/N59021PM

Sugden, D. E., McCulloch, R. D., Bory, A. J.-M., & Hein, A. S. (2009). Influence of Patagonian glaciers on Antarctic dust deposition during the last glacial period. *Nature Geoscience*, *2*(4), 281–285. https://doi.org/10.1038/NGEO474

Sushchevskaya, N., Migdisova, N., Antonov, A., Krymsky, R. S., Belyatsky, B., Kuzmin, D., & Bychkova, Y. V. (2014). Geochemical features of the quaternary lamproitic lavas of Gaussberg Volcano, East Antarctica: Result of the impact of the Kerguelen plume. *Geochemistry International*, *52*(12), 1030–1048. https://doi.org/10.1134/s0016702914120106

Tanaka, T., Togashi, S., Kamioka, H., Amakawa, H., Kagami, H., Hamamoto, T., et al. (2000). JNdi-1: A neodymium isotopic reference in consistency with LaJolla neodymium. *Chemical Geology*, *168*(3–4), 279–281. https://doi.org/10.1016/s0009-2541(00)00198-4

Taylor, K. C., Alley, R. B., Meese, D. A., Spencer, M., Brook, E., Zielinski, G., et al. (2004). Dating the Siple Dome, Antarctica ice core by manual and computer interpretation of annual layering. *Journal of Glaciology*, *50*(170), 453–461. https://doi.org/10.3189/172756504781829864

Toggweiler, J. R., Russell, J. L., & Carson, S. R. (2006). Midlatitude westerlies, atmospheric $CO_2$, and climate change during the ice ages. *Paleoceanography*, *21*(PA2005). https://doi.org/10.1029/2005PA001154

Wendler, G., Stearns, C., Weidner, G., Dargaud, G., & Parish, T. (1997). On the extraordinary katabatic winds of Adélie Land. *Journal of Geophysical Research: Atmospheres*, *102*(D4), 4463–4474. https://doi.org/10.1029/96jd03438

Winton, V. H. L., Dunbar, G. B., Atkins, C. B., Bertler, N. A. N., Delmonte, B., Andersson, P. S., et al. (2016). The origin of lithogenic sediment in the south-western Ross Sea and implications for iron fertilization. *Antarctic Science*, *28*(4), 250–260. https://doi.org/10.1017/S095410201600002X

Wu, Y., Pena, L., Goldstein, S., Basak, C., Bolge, L., Jones, K., et al. (2020). A user-friendly workbook to facilitate rapid and accurate rare Earth element analyses by ICP-MS for multispiked samples. *Geochemistry, Geophysics, Geosystems*, *21*(9), e2020GC009042. https://doi.org/10.1029/2020gc009042

Xia, Z., Yu, Z., & Loisel, J. (2018). Centennial-scale dynamics of the Southern Hemisphere westerly Winds across the Drake Passage over the past two millennia. *Geology*, *46*(10), 855–858. https://doi.org/10.1130/g40187.1